Available online at www.sciencedirect.com
SCIENCE DIRECT®
Surface Science 523 (2003) 80–88
SURFACE SCIENCE
www.elsevier.com/locate/susc

Island formation on 0.1 at.% La-doped $SrTiO_3(1\,0\,0)$ at elevated temperatures under reducing conditions

A. Gunhold [a], L. Beuermann [a], M. Frerichs [a], V. Kempter [a], K. Gömann [b], G. Borchardt [b], W. Maus-Friedrichs [a,*]

[a] *Institut für Physik und Physikalische Technologien, Technischen Universität Clausthal, Leibnizstrasse 4, D-38678 Clausthal-Zellerfeld, Germany*

[b] *Institut für Metallurgie, Technischen Universität Clausthal, Robert-Koch-Strasse 42, D-38678 Clausthal-Zellerfeld, Germany*

Received 9 July 2002; accepted for publication 11 September 2002

Abstract

Annealing of 0.1 at.% La-doped $SrTiO_3(1\,0\,0)$ under reducing conditions ($p_{O_2} \leqslant 10^{-8}$ mbar) between 1000 and 1300 °C for 2 h leads to the formation of islands, which coalesce yielding agglomerates with characteristic dimensions of several micrometers after 40 h. Microscopic (scanning electron microscopy, scanning tunneling microscopy) and spectroscopic techniques (metastable impact electron spectroscopy, ultraviolet photoelectron spectroscopy, scanning tunneling spectroscopy, depth profile Auger electron spectroscopy) were used to reveal the reaction mechanism. Under these experimental conditions the sublimation of titanium from the surface takes place. The islands contain only Ti (40 at.%) and O (60 at.%). They show metallic-like behaviour and consist of Ti_2O_3. The island formation results from the creation of oxygen vacancies on the surfaces followed by a Ti depletion in the surface region up to a depth of about 8 nm.

Keywords: Visible and ultraviolet photoelectron spectroscopy; Metastable induced electron spectroscopy (MIES); Auger electron spectroscopy; Scanning electron microscopy; Scanning tunneling microscopy; Scanning tunneling spectroscopies; Surface structure, morphology, roughness, and topography; Alkaline earth metals

1. Introduction

The surfaces of $SrTiO_3$ single crystals have been investigated previously because of their relevance in sensor applications, in photocatalysis, as substrates for the epitaxial growth of high-T_c superconductors or as dielectric gate in silicon-based electronic devices [1–7]. During the heat treatment of $SrTiO_3$ single crystals in an oxygen rich atmosphere the appearance of SrO phases has been reported [5,8–11]. This SrO formation is observed for donor doped, undoped and acceptor doped $SrTiO_3(1\,0\,0)$ surfaces for different dopant concentrations.

The mechanisms leading to Sr enhancement on $SrTiO_3$ surfaces were described within the framework of point defect chemistry formalism: the Schottky equilibrium requires the product of Sr

* Corresponding author. Tel.: +49-5323-722310; fax: +49-5323-723600.
E-mail address: wmf@physik.tu-clausthal.de (W. Maus-Friedrichs).

0039-6028/02/$ - see front matter © 2002 Elsevier Science B.V. All rights reserved.
PII: S0039-6028(02)02402-0

vacancies and oxygen vacancies to be constant at a certain temperature. Under oxidizing conditions, the ambient atmosphere acts as an oxygen source providing a low oxygen vacancy concentration in the bulk and, according to the Schottky equilibrium, a large number of Sr vacancies (see [12] and references therein). This Sr vacancy formation in the bulk results in a Sr enrichment on the surface leading to the observed SrO island formation and to the desorption of Sr from the surface [9].

In contrast, under reducing conditions the formation of TiO_x phases ($1 \leqslant x \leqslant 2$) appearing on undoped $SrTiO_3(1\,0\,0)$ surfaces at about 1000 °C after 20 h was reported [5,8]. On undoped $SrTiO_3(1\,1\,0)$ also Ti-rich metallic phases have been observed appearing at temperatures between 800 and 1200 °C [13].

Very recently, a number of reconstructions were reported by M. Castell which appear during the very first stage of island formation on weakly donor doped $SrTiO_3(1\,0\,0)$ surfaces heated under vacuum conditions [14]. These reconstructions result in the formation of nanolines and nanodots after prolonged heating [15] which constitute the first steps in the formation of nanocrystalline islands as will be shown later.

A consistent model explaining both the observations for oxidizing and reducing conditions is still lacking. It is the aim of this work to extend the available investigations for donor doped $SrTiO_3$ surfaces annealed under vacuum conditions by combining microscopic and spectroscopic methods.

Secondary electron microscopy (SEM) and scanning tunneling microscopy (STM) are applied to investigate the changes of the surface structure during heating. STM is limited to fields of view below about 4 μm and island heights below 150 nm. SEM provides a lateral resolution of about 500 nm and a field of view up to 100 μm. The combination of both techniques gives us the opportunity to investigate a wide range of island sizes.

Auger electron spectroscopy (AES), metastable impact electron spectroscopy (MIES), ultraviolet photoelectron spectroscopy (UPS), and scanning tunneling spectroscopy (STS) are applied to investigate the chemical composition and the electronic structure of the surface. AES, combined with SEM in the same apparatus, provides furthermore depth profile analysis due to its combination with a sputter gun. It allows spot analysis with lateral resolution of about 2–3 μm. MIES and UPS have already provided information about the surface density of states (SDOS) and the bulk density of states (BDOS) of $SrTiO_3(1\,0\,0)$, respectively [16]. MIES is an extremely surface sensitive technique because the resulting electron emission is caused by the interaction of the He^* atoms with the outermost part of the wave functions of the surface [17,18]. STS, being combined with STM, also provides information on the outermost part of the surface wave functions, but with lateral resolution. STS provides information on the occupied and unoccupied states of the surface. However, STS is restricted to a range of about ±4 eV around the Fermi level [19].

2. Experimental

The measurements have been performed in three different apparatuses. AES and SEM are performed in an ultrahigh vacuum chamber with a base pressure of 2×10^{-10} mbar. It is equipped with a commercial AES/SEM system (Physical Electronics) and a sputter gun for depth profile analysis. MIES and UPS experiments are performed in a second apparatus which has been described in detail previously [20]. It provides a base pressure of 2×10^{-11} mbar. Besides the hemispherical analyzer (VSW HA 100) it consists of a He^* source with a time-of-flight technique to separate electrons emitted by He^* (MIES) and HeI (UPS) interaction with the surface. Therefore, MIES and UPS spectra are collected simultaneously [20]. The spectra are recorded with a resolution of 250 meV under normal emission within 100 s. The angle of incidence for the mixed He^*/HeI beam is 45°. The MIES and UPS spectra are displayed as a function of the electron binding energy referring to the Fermi level, although this is ambiguous for MIES spectra not resulting from the Auger deexcitation (AD) process [17]. STM and STS measurements are performed in a third apparatus with a base pressure of 4×10^{-10} mbar in its microscope chamber and below 1×10^{-9} mbar in its main chamber. It is equipped with a

commercial AFM/STM system (Omicron AFM/STM).

Polished 0.1 at.% La-doped $SrTiO_3(1\,0\,0)$ crystals (Crystec) with a size of $10 \times 10 \times 1$ mm^3 for spectroscopic measurements and $5 \times 5 \times 0.5$ mm^3 for microscopic measurements were investigated. All crystals were heated to about 800 °C at pressures below 1×10^{-8} mbar for 10–30 min prior to the investigations, thus removing surface contaminants completely. The surface cleanness was checked by XPS and MIES measurements. The target temperature was controlled by a commercial optical pyrometer (Impac IGA 120) through view ports in all cases.

The heating procedures in the STM/AFM and the MIES/UPS apparatus are reproduced with a precision of ±10 °C. AES/SEM measurements were performed on crystals being heated either in the MIES/UPS apparatus or in the STM/MIES apparatus. This may cause possible alterations of the surface conditions due to the ex situ transport. All analyses and characterizations were performed at room temperature.

3. Results

During all heating procedures inside the MIES/UPS apparatus molybdenum targets were mounted opposite to our samples in a distance of several cm. Subsequent Auger analysis of these Mo plates showed that Ti sublimated from the $SrTiO_3$ surfaces. Sr could not be found at all. We are not able to quantify the amount of Ti desorbed from the $SrTiO_3$ surfaces.

Fig. 1 shows a STM picture (500×500 nm^2) of the 0.1 at.% La-doped $SrTiO_3(1\,0\,0)$ surface heated at 1000 °C for 5 h under reducing conditions (pressures below 1×10^{-8} mbar). The step heights are about 3 Å (60%), 6 Å (30%) and 9 Å and higher (10%). These heights do not correspond to the step height of $SrTiO_3$ in [0 0 1] direction [21]. Szot et al. reported the formation of TiO_x ($1 \leqslant x \leqslant 2$) phases on such surfaces. We therefore attribute the observed step heights to these phases as TiO_2 would display a step height of 2.96 Å [21]. The step density amounts to about 100 nm^{-1} corresponding to a miscut angle of about 0.25°.

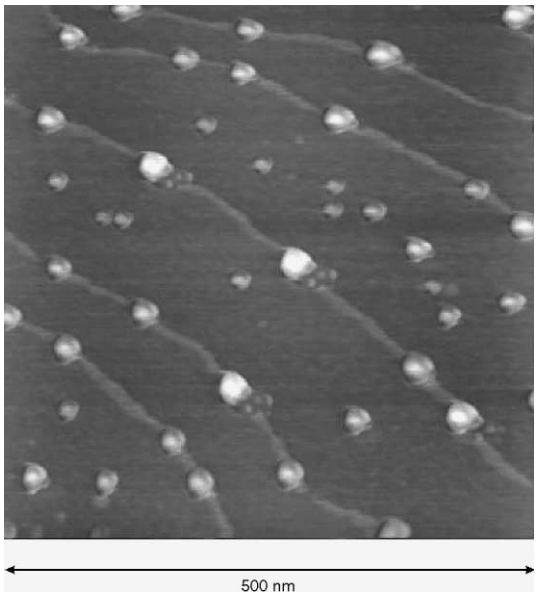

Fig. 1. STM image (500×500 nm^2) for 0.1 at.% La-doped $SrTiO_3(1\,0\,0)$ heated at 1000 °C for 5 h under reducing conditions; gap voltage + 2.5 V/tunneling current 0.5 nA.

On top of the surfaces, some islands appear (white spots) with typical sizes between 10 and 20 nm. The islands cover (7 ± 1)% of the surface.

Fig. 2 shows a STM picture (2000×2000 nm^2) of the $SrTiO_3(1\,0\,0)$ surface held at 1300 °C for 25 h. The number of islands has drastically increased as compared to Fig. 1. The island size varies typically between 20 and 200 nm. Larger islands appear also, but could not be analyzed in detail applying STM due to its limitation to step heights below 150 nm. The steps on the surface are not well resolved because of the large island heights.

Fig. 3 shows (on the left-hand side) an SEM image (100×100 μm^2) of the $SrTiO_3(1\,0\,0)$ surface held at 1300 °C for 40 h (denoted by (a)). Most of the small islands observed for shorter heating (see Figs. 1 and 2) have agglomerated forming large islands. On this surface in situ AES analysis was performed at the spot positions indicated in the SEM image. All AES spectra are weighted by the respective sensitivity factors of Sr, Ti, O and La. The depth profile analysis (Fig. 3(b)) performed between the islands clearly shows a Ti depletion in the surface region. At a depth of about 8 nm the

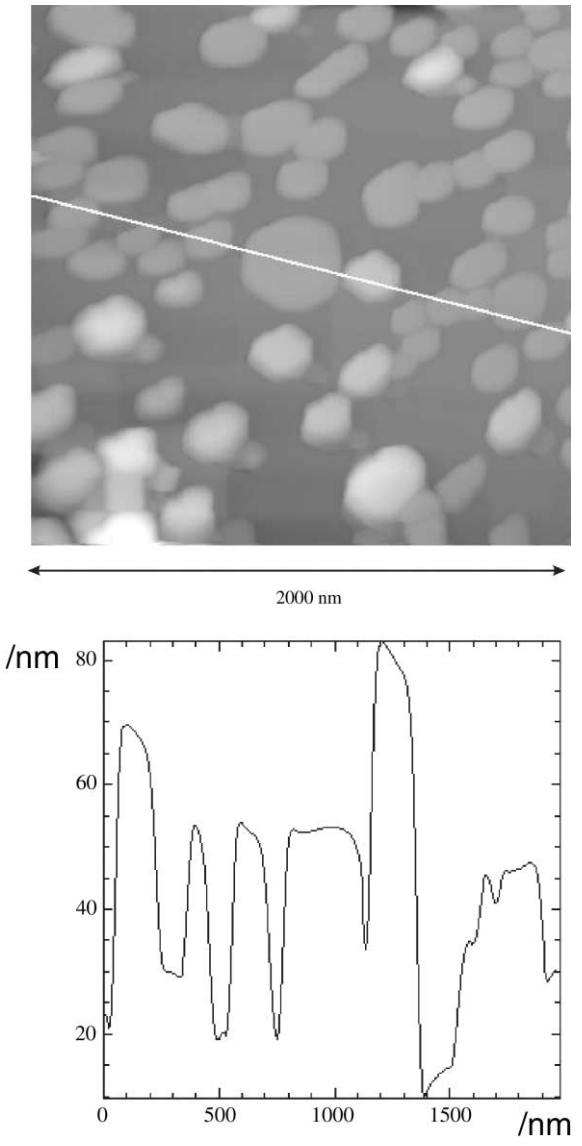

Fig. 2. STM image (2000×2000 nm^2) for 0.1 at.% La-doped $SrTiO_3$(1 0 0) heated at 1300 °C for 25 h under reducing conditions; gap voltage + 1.5 V/tunneling current 0.5 nA.

chemical composition reaches the stoichiometric composition of $SrTiO_3$. Fig. 3(c) shows the AES measurement performed on the islands as indicated in Fig. 3(a). In contrast to (b) it shows almost no contribution from Sr, but Ti and O are found (the positions where Sr peaks should appear are marked in Fig. 3(c)). We estimated the stoichiometry of these islands taking into account the respective sensitivity factors and found them to consist of (39.1 ± 1.5) at.% Ti and (60.9 ± 1.5) at.% O, which suggests that the islands consist of Ti_2O_3.

Fig. 4 shows MIES (a) and UPS (b) spectra of the $SrTiO_3$(1 0 0) surface heated at 1000 °C as indicated. The surface work function, which can be derived from the low energy onset in the UPS spectra, is 4.2 to 2.4 eV after heating. As is shown in [16], the MIES spectrum is mainly due to Auger neutralization (AN) involving O 2p and Ti 3d electrons. The large peaks at high binding energies are caused by secondary electrons and in MIES additionally by AN involving two O(2p) electrons; this part of the spectrum will not be discussed here. Because the Ti^{3+} 3d species form a rather narrow band, the MIES spectrum in the range $4 \leqslant E_B \leqslant 9$ eV is rather similar to an AD spectrum, but shifted to higher binding energies by 1.2 eV [16]. In order to compare MIES, UPS and STS, the MIES spectra of Fig. 4(a) are shifted towards lower binding energies by this value.

The spectra for the unheated crystal are identical with the MIES [16] and UPS [11,16,22] spectra for $SrTiO_3$(1 0 0). It has been shown previously, that Ruddlesden–Popper phases $Sr_{n+1}Ti_nO_{3n+1}$(1 0 0) ($1 \leqslant n \leqslant 3$) show MIES and UPS spectra that are very similar to the ones for $SrTiO_3$(1 0 0) surfaces [11]. The prominent structures at $E_B = 5.2$ eV in MIES and $E_B = 5.0$ and 7.1 eV in UPS are due to the electron emission from O(2p). In addition, both MIES and UPS show the development of a peak at the Fermi level. In MIES it is found at a binding energy of $E_B = 0.6$ eV. In UPS the peak appears to consist of a doublet $E_B = 0.6$ and 1.2 eV as visible in the inset, although the evaluation is ambiguous due to the statistics of the data. The peaks have saturated already after 5 h at 1000 °C. The UPS peak at $E_B = 1.0$ eV was attributed previously to occupied Ti 3d orbitals at Ti^{3+} 3d reduced cations of the bulk [22,23]. $SrTiO_3$(1 0 0) surfaces without islands did not show contributions below $E_B \approx 3$ eV with MIES [16]. We therefore attribute the MIES and UPS peak at $E_B = 0.6$ eV to the islands seen with STM. From the relative peak areas we estimate that the island coverage of the surface is about 5%; from STM images a value of about 7% was obtained (see Fig. 1).

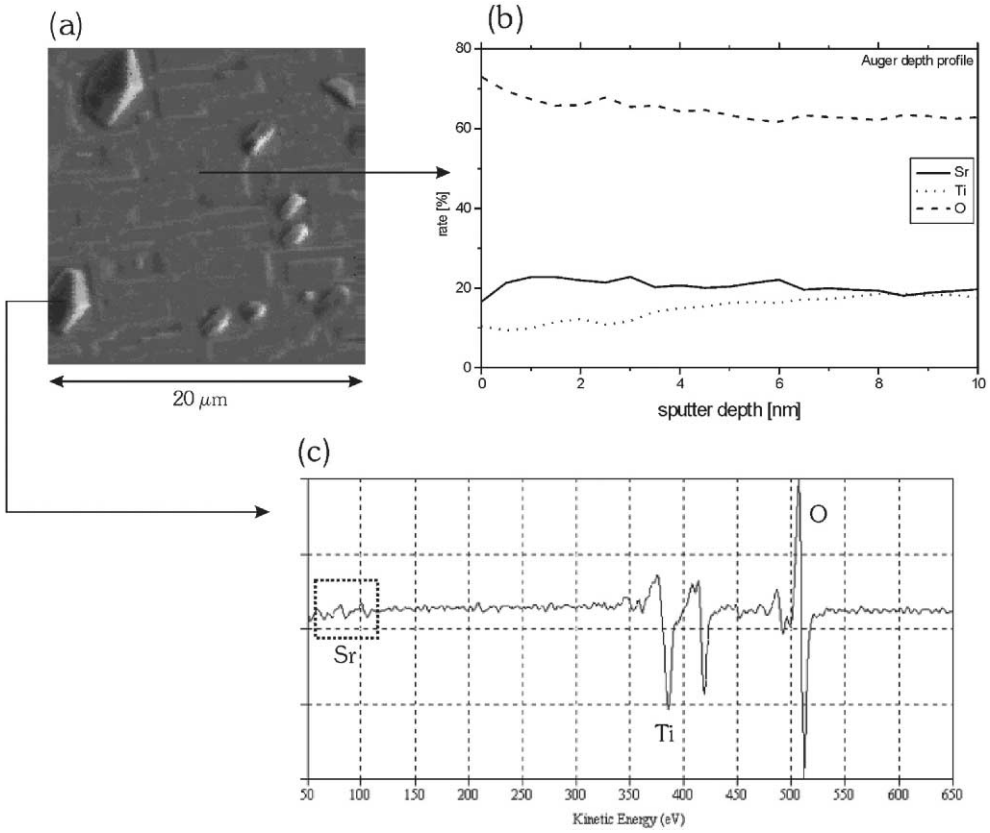

Fig. 3. SEM image (1000×1000 nm^2) (a) and AES spectra for 0.1 at.% La-doped $SrTiO_3$(1 0 0) heated at 1300 °C for 40 h under reducing conditions; the AES depth profile analysis (b) and the AES spectrum (c) are recorded at the indicated positions.

Fig. 5 shows STS spectra (I/V curves (a) and dI/dV curves (b)) observed from a region between the islands and from islands as shown in Fig. 2. Similar spectra are found for all investigated 0.1 at.% La-doped and undoped $SrTiO_3$-(1 0 0) surfaces heated under reducing conditions for different durations. The results are compared with those for the clean unheated 0.1 at.% La-doped $SrTiO_3$ (1 0 0) surface prior to any annealing procedure. The spectrum for the pure surface corresponds well to the pure $SrTiO_3$ surface: it shows a band gap of 3.2 eV and its Fermi level is pinned to the conduction band minimum due to the donor doping and intrinsic Schottky defects [24]. The weak intensity between about −0.1 and −2 eV is apparently induced by occupied Ti 3d orbitals resulting from defects [16]. Nevertheless, the conductance spectrum (Fig. 5(b)) shows, that this surface is insulating because $dI/dU = 0$ at the Fermi level ($U = 0$). Between the islands also an insulating behaviour is observed with a band gap of 3.2 eV between the valence band maximum and the Fermi level. In contrast, STS from the islands shows metallic behaviour as can be seen from the fact, that $I(U)$ crosses the Fermi level with a finite slope. We therefore assume that the MIES signal visible at E_F is induced by these islands. From the AES measurements it was found that the large islands possess the stoichiometry of Ti_2O_3 which exhibits occupied Ti 3d orbitals near E_F. These islands are responsible for structures near E_F in MIES and STS. We therefore assume that all observed islands consist of Ti_2O_3.

The same kind of microscopic and spectroscopic measurements were also performed for

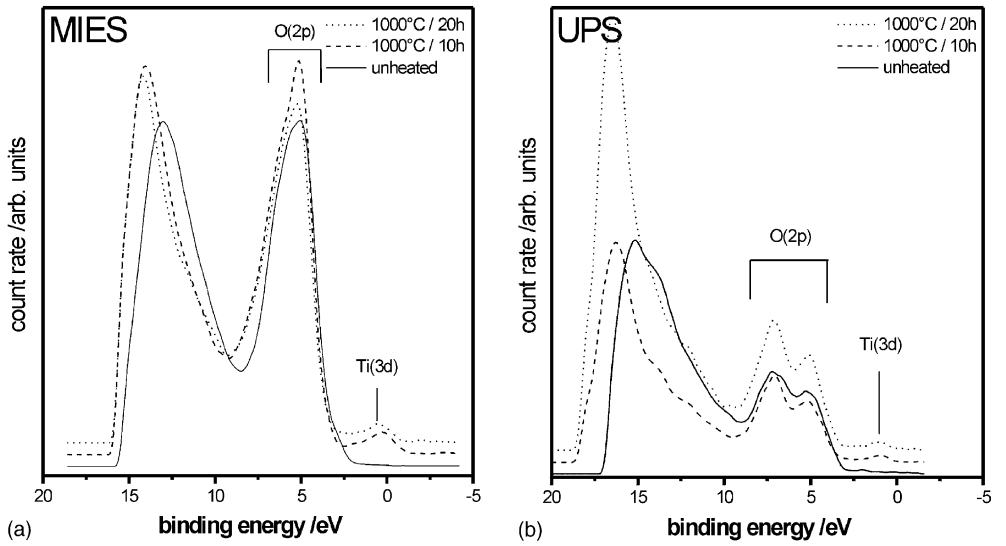

Fig. 4. MIES (a) and UPS (b) spectra for 0.1 at.% La-doped $SrTiO_3(1\,0\,0)$ heated at 1000 °C under reducing conditions.

undoped $SrTiO_3(1\,0\,0)$. The results are similar to those for 0.1 at.% La-doped $SrTiO_3(1\,0\,0)$.

4. Discussion

The appearance of SrO complexes on top of donor doped $SrTiO_3(1\,0\,0)$ surfaces at elevated temperatures under oxidizing conditions has been analyzed in detail previously by Szot et al. [5,8,9]. It can be understood within the framework of a point defect chemistry description (see [12] for an introduction). Because of the high oxygen partial pressure $p(O_2)$ in ambient atmosphere oxygen vacancies will not be present at sufficiently high temperature. Therefore, the donor $D^{\cdot}$ will almost completely be compensated by strontium vacancies V''_{Sr} [24,25] (we will apply the notation of Kröger and Vinck [26] to describe defects) [12]:

$$2 \cdot [V''_{Sr}] \approx [D^{\cdot}] \tag{1}$$

In contrast, under reducing conditions the number of oxygen vacancies $V^{\cdot\cdot}_{O}$ will be very high because of the low ambient $p(O_2)$:

$$O^{x}_{O} \rightarrow V^{\cdot\cdot}_{O} + 2e' + \tfrac{1}{2}O_2 \uparrow \tag{2}$$

(O^{x}_{O} denotes an oxygen atom on a regular lattice site.)

$(1\,0\,0)$ oriented $SrTiO_3$ single crystals consist of alternating layers of SrO and TiO_2. The crystal surfaces are terminated by TiO_2 either completely [27] or at least to about 80% [28,29] in order to minimize their surface energy [30]. Heating undoped $SrTiO_3(1\,0\,0)$ surfaces in ultrahigh vacuum results in the formation of a completely TiO_2 terminated surface and the formation of oxygen vacancies at the surface [14,27,31]. These vacancies produce a UPS peak at a binding energy of $E_B = 1.3$ eV [27,31] which is due to the peak centered at $E_B = 1.2$ eV in our UPS data. For $TiO_2(1\,0\,0)$ surfaces the formation of oxygen vacancies at elevated temperatures is also well known [22].

We assume that on TiO_2 terminated $SrTiO_3(1\,0\,0)$ surfaces the formation of oxygen vacancies leads to the formation of Ti vacancies and herewith a Schottky-like disorder in the $SrTiO_3$ lattice. The Ti vacancy formation is responsible for the observed sublimation of Ti from the surface.

This assumption is able to explain the observed Ti_2O_3 enrichment on top of the $SrTiO_3(1\,0\,0)$

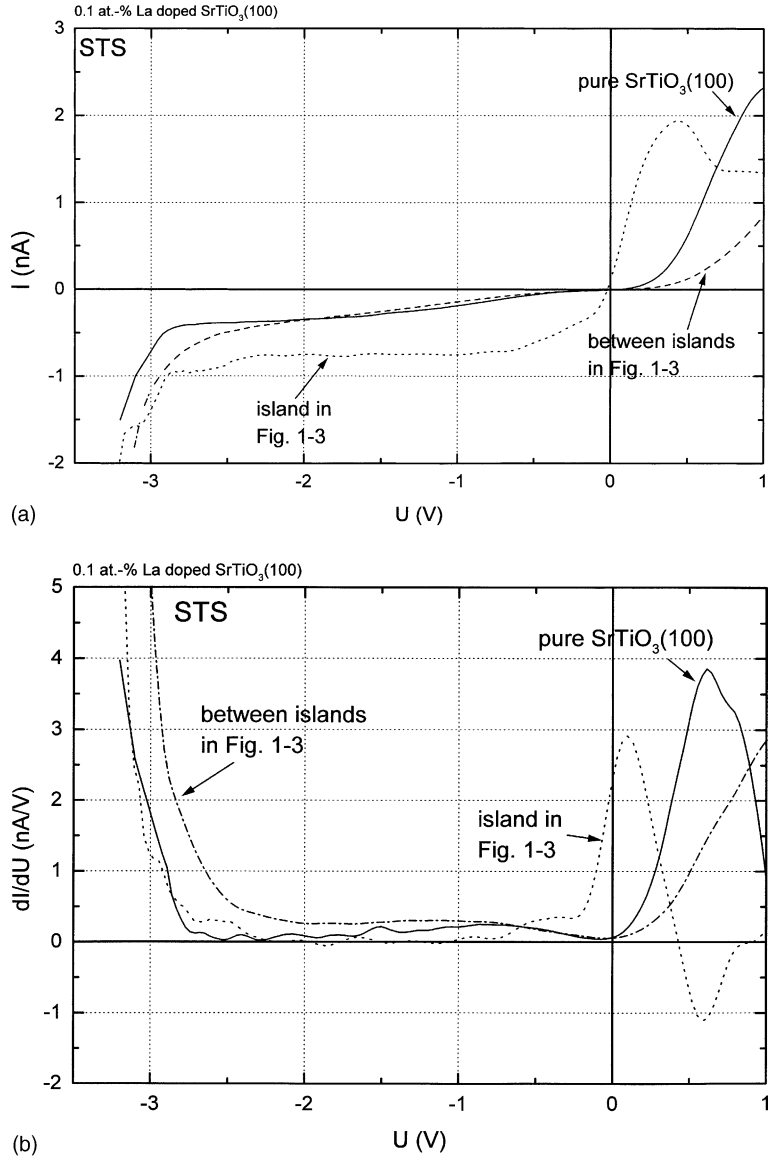

Fig. 5. STS spectra (I/V) (a) and conductance spectra ($\mathrm{d}I/\mathrm{d}V$) (b) from a clean $SrTiO_3(1\,0\,0)$ surface and from regions of the heated 0.1 at.% La-doped $SrTiO_3(1\,0\,0)$ surface between the islands and on top of the islands in Fig. 2.

surfaces as well as the Ti sublimation from the surface:

$$3\mathrm{Ti}_{\mathrm{Ti}}^{x} + 6\mathrm{O}_{\mathrm{O}}^{x} \rightarrow 3\mathrm{V}_{\mathrm{Ti}}'''' + 6\mathrm{V}_{\mathrm{O}}^{\cdot\cdot} + \tfrac{3}{2}\mathrm{O}_2 \uparrow + \mathrm{Ti}_2\mathrm{O}_3 + \mathrm{Ti} \uparrow \quad (3)$$

The metallic behaviour of the islands as observed with MIES and STS results from the occupied Ti 3d level of Ti_2O_3. The Ti depletion reaches about 8 nm into the crystal as shown by the AES results in Fig. 3(b). On the surface Ti_2O_3 complexes seem to be mobile, thus agglomerating to large islands during prolonged heating. Nevertheless, MIES and STS peaks from these islands display rather different features: the MIES peak located at $E_B = 0.6$ eV

possesses a FHWM of about 2 eV. In contrast, the peak in dI/dU at E_F is only about 0.2 eV wide. This difference is not understood up to now and requires additional studies.

Recently Castell has published results from 0.5 at.% Nb-doped $SrTiO_3(1\,0\,0)$ surfaces heated up to 1400 °C under ultrahigh vacuum conditions. He observed several reconstructions during the different heat treatments. Heating the crystal up to 870 °C leads initially to nanolines in zig-zag or square configuration. Further annealing transforms the nanolines to nanodots and at temperatures above approximately 1200 °C these nanostructures disappear and a $c(4 \times 2)$ reconstructured surface [14,15] emerges. We assume that these nanostructures represent the first step in the formation of the islands observed here. Obviously the well-structured nanostructures agglomerate during prolonged heating.

5. Summary

Under reducing conditions (below 1×10^{-8} mbar) on 0.1 at.% La-doped $SrTiO_3(1\,0\,0)$ single crystal surfaces islands are formed consisting of titanium (40 at.%) and oxygen (60 at.%) at temperatures between 1000 and 1300 °C. Furthermore, the sublimation of Ti from these surfaces under these conditions is observed.

Ti_2O_3 is agglomerated in large islands (typical sizes of several μm) showing metallic-like character due to its occupied Ti 3d orbitals, while Ti depletion between the islands is found. From depth profile analysis a depletion zone of about 8 nm is found underneath the surface before the bulk reaches its stoichiometric composition.

We propose a mechanism accounting for the influence of surface oxygen vacancies produced under reducing conditions at elevated temperatures. These vacancies lead to the reduction of Ti and the formation of Ti vacancies. The excess Ti sublimates or forms Ti_2O_3 crystallites at the surface.

Acknowledgements

Financial support by the Deutsche Forschungsgemeinschaft under contracts Ma 1893/2 and Bo 532/47 is gratefully acknowledged. The authors thank P. Cyris for AES and SEM measurements. Furthermore, we wish to thank Dr. M.R. Castell for helpful discussions.

References

[1] V. Ravikumar, D. Wolf, V.P. David, Physical Review Letters 74 (1995) 174.
[2] B. Stäuble-Pümpin, B. Ilge, V.C. Matijasevic, P.M.L.O. Scholte, A.J. Steinfort, F. Tuinstra, Surface Science 369 (1996) 313.
[3] T. Matsumoto, H. Tanaka, T. Kawai, S. Kawai, Surface Science Letters 278 (1992) L153.
[4] Y. Liang, D.A. Bonnell, Surface Science Letters 285 (1993) L510.
[5] K. Szot, W. Speier, J. Herion, Ch. Freiburg, Applied Physics A 64 (1997) 55.
[6] A. Lopez, T. Heller, T. Bitzer, Q. Chen, N.V. Richardson, Surface Science Letters 494 (2001) L811.
[7] R.A. McKee, F.J. Walker, M.F. Chrisholm, Physical Review Letters 81 (1998) 3014.
[8] K. Szot, W. Speier, Physical Review B 60 (1999) 5909.
[9] K. Szot, W. Speier, U. Breuer, R. Meyer, J. Szade, R. Waser, Surface Science 460 (2000) 112.
[10] H. Wei, L. Beuermann, J. Helmbold, G. Borchardt, V. Kempter, G. Lilienkamp, W. Maus-Friedrichs, Journal of the European Ceramic Society 21 (2001) 1677.
[11] H. Wei, W. Maus-Friedrichs, G. Lilienkamp, V. Kempter, J. Helmbold, K. Gömann, G. Borchardt, Journal of Electroceramics 8 (2002) 221.
[12] W. Menesklou, H.-J. Schreiner, K.H. Härdtl, E. Ivers-Tiffée, Sensors and Actuators B 59 (1999) 184.
[13] H. Bando, Y. Aiura, T. Shimizu, Y. Ochiai, Y. Haruyama, Y. Nishihara, Journal of Electron Spectroscopy and Related Phenomena 114–116 (2001) 313.
[14] M.R. Castell, Surface Science 505 (2002) 1.
[15] M.R. Castell, Surface Science 516 (2002) 33.
[16] W. Maus-Friedrichs, M. Frerichs, A. Gunhold, S. Krischok, V. Kempter, G. Bihlmayer, Surface Science 515 (2002) 499.
[17] H. Morgner, Advances in Atomic, Molecular, and Optical Physics 48 (2000) 387.
[18] Y. Harada, S. Masuda, H. Ozaki, Chemical Reviews 97 (1997) 1897.
[19] R. Wiesendanger, Scanning Probe Microscopy and Spectroscopy, Cambridge University Press, Cambridge, MA, 1994.
[20] M. Brause, B. Braun, D. Ochs, W. Maus-Friedrichs, V. Kempter, Surface Science 398 (1998) 184.
[21] R.W.G. Wyckoff, Crystal Structures, vol. 2, 2nd ed., Interscience Publishers, 1964.
[22] V.E. Henrich, P.A. Cox, The Surface Science of Metal Oxides, Cambridge University Press, Cambridge, 1994.

[23] B. Cord, R. Courths, Surface Science 162 (1985) 34.
[24] R. Moos, K.H. Härdtl, Journal of the American Ceramic Society 80 (1997) 2549.
[25] M.J. Akhtar, Z.-U.-N. Akhtar, R.A. Jackson, C.R.A. Catlow, Journal of the American Ceramic Society 78 (1995) 421.
[26] F.A. Kröger, H.J. Vink, Solid State Physics 3 (1956) 307.
[27] A. Hirata, K. Saiki, A. Koma, A. Ando, Surface Science 319 (1994) 267.
[28] T. Nishimura, A. Ikeda, H. Nambe, T. Morishita, Y. Kido, Surface Science 421 (1999) 273.
[29] G. Charlton, S. Brennan, C.A. Muryn, R. McGradth, D. Norman, T.S. Turner, G. Thornton, Surface Science Letters 457 (2000) L376.
[30] P.A.W. van der Heide, Q.D. Jiang, Y.S. Kim, J.W. Rabalais, Surface Science 473 (2001) 59.
[31] A. Hirata, A. Ando, K. Saiki, A. Koma, Surface Science 310 (1994) 89.